

# Stability and Lifetime of Antiferromagnetic Skyrmions

P. F. Bessarab,<sup>1,2</sup> D. Yudin,<sup>2</sup> D. R. Gulevich,<sup>2</sup> P. Wadley,<sup>3</sup> M. Titov,<sup>4,2</sup> and Oleg A. Tretiakov<sup>5,\*</sup>

<sup>1</sup>*Science Institute of the University of Iceland, 107 Reykjavík, Iceland*

<sup>2</sup>*ITMO University, Saint Petersburg 197101, Russia*

<sup>3</sup>*School of Physics and Astronomy, University of Nottingham, Nottingham NG7 2RD, United Kingdom*

<sup>4</sup>*Radboud University Nijmegen, Institute for Molecules and Materials, NL-6525 AJ Nijmegen, The Netherlands*

<sup>5</sup>*Institute for Materials Research, Tohoku University, Sendai 980-8577, Japan*

The two-dimensional Heisenberg exchange model with out-of-plane anisotropy and Dzyaloshinskii-Moriya interaction is employed to investigate the lifetime and stability of antiferromagnetic (AFM) skyrmion as a function of temperature and external magnetic field. An isolated AFM skyrmion is shown to be metastable at zero temperature in a certain parameter range set by two boundaries separating the skyrmion state from the uniform AFM phase and a stripe domain state. The distribution of the energy barriers for the AFM skyrmion decay into the uniform AFM state complements the zero-temperature stability diagram and demonstrates that the skyrmion stability region is significantly narrowed at finite temperatures. We show that the AFM skyrmion stability can further be enhanced by an application of magnetic field, which strength is comparable with the spin-flop field. This stabilization of AFM skyrmions in external magnetic fields is in sharp contrast to the behavior of their ferromagnetic counterparts. Furthermore, we demonstrate that the AFM skyrmions are stable on the timescales of milliseconds below 50 K for realistic material parameters, making it feasible to observe them in modern experiments.

*Introduction.* Certain types of non-linear sigma models support topologically non-trivial ground states which turn out to be robust with respect to smooth variations of the model parameters. Such ground states are characterized by topological invariants, while their stability is guaranteed by a generalized Hobart–Derrick criterion [1]. One well-known example of such a model has been provided by Skyrme in the context of high energy physics [2]: he treated nucleon as a vortex state of pion matter. To study the problem Skyrme suggested a non-linear sigma model with terms linear in spatial gradients. The corresponding classical equations of motion give rise to topologically non-trivial solutions – skyrmions that are characterized by a non-trivial topological invariant known as the topological charge.

Nowadays, a wide range of non-collinear magnetic configurations ranging from magnetic bubbles to helical spiral states are routinely observed in low-dimensional magnetic structures. The direct analogy with the original Skyrme model has been utilized to predict a particle-like topological magnetic texture, currently referred to as magnetic skyrmion [3]. The experimental observation of magnetic skyrmions in films of cubic helimagnets [4] and ultrathin ferromagnetic films interfaced with heavy metals [5, 6] resulted in extensive theoretical and experimental efforts to study their peculiar topological properties and potentially fast dynamics [7]. For future technological applications, a lot of work has also been devoted to controllable creation [8–10] and annihilation of the skyrmions [11].

A keen interest in skyrmion dynamic properties is stimulated by their potential use in the next-generation spintronic devices [12, 13]. Currently ferromagnetic (FM) skyrmions have been found both as a ground state forming lattices in cubic helimagnets [14, 15] and as

metastable but long-lived states in ferromagnet/heavy-metal multilayers [14, 16–22]. The latter are often discussed as elements of skyrmionic racetrack memory [23–26], but suffer from the skyrmion Hall effect. This effect may be easily understood using collective coordinate approach to topological spin textures [27–29], where it translates into a generalized gyrotropic (Magnus) force [24, 30–32] acting on a skyrmion in the transverse to the applied electric current direction, and thus eventually pushing it over the edge of nanotrack, potentially limiting the use of skyrmions for racetrack nanodevices [23].

It has recently been suggested based on both analytical arguments and micromagnetic simulations that unfavorable effect of the topological Magnus force can completely cancel out in chiral antiferromagnetic (AFM) skyrmions [33–35]. In such AFM skyrmions, the Magnus force on one magnetic sublattice is equal in magnitude but has an opposite sign to the one on the other sublattice, thus leading to straight skyrmion trajectories along the applied current and furthermore greatly enhanced velocities compared to its FM counterpart [33–36]. Additionally, using micromagnetic simulations it has been proposed how to create the AFM skyrmions by injecting vertically spin-polarized current into a nanodisc with uniform AFM state [34]. A possible experimental realization of an isolated skyrmion as well as skyrmion lattice has been suggested by using a standard bipartite lattice in which each sublattice supports a skyrmion crystal (e.g, honeycomb lattice) coupled to an AFM [37]. Moreover, the topological spin Hall effect has been studied in AFM skyrmions and its impact on the current-induced motion has been demonstrated [38, 39].

Even though there is an enormous progress in studying the dynamics of AFM spin textures [40–43] and AFM ma-

materials in general [44, 45], the AFM skyrmions have not been experimentally discovered yet. This may have to do with the overall challenge in detection of Néel-order spin textures [46], on top of finding appropriate chiral AFM material with the parameters in the range satisfying the AFM skyrmion (meta)stability [33]. The lifetime of AFM skyrmions could also be an issue, as they are metastable states of the system. If the lifetime is too short on a scale of available experimental techniques, such as spin-polarized scanning-tunneling microscopy (SP-STM) or magnetic exchange force microscopy [47], the AFM skyrmion would decay before being detected.

In this Letter, we analyze stability of AFM skyrmions, an essential prerequisite for their use in applications. Both the activation energy for the skyrmion decay and the skyrmion lifetime are evaluated as functions of material parameters, temperature, and magnetic field using harmonic transition state theory for spins [48]. This analysis makes it possible to quantify the skyrmion stability at macroscopic time scales. We complement the zero-temperature stability diagram for an isolated AFM skyrmion with the distribution of energy barriers for the skyrmion collapse into the uniform AFM phase. Our analysis demonstrates that the stability region may be significantly narrowed even at small temperatures. However, the AFM skyrmions can be further stabilized by external magnetic fields, which is in sharp contrast to their FM counterparts. The AFM skyrmions are shown to be rather stable at temperatures of 50 K and below for typical AFMs, where they may be detected experimentally using modern techniques for the detection of Néel order parameter [46].

*Methods.* We study a monolayer AFM spin system on a square lattice using localized-moment Hamiltonian equipped with Heisenberg exchange coupling, antisymmetric Dzyaloshinskii-Moriya interaction (DMI), out-of-plane anisotropy, and Zeeman term. The energy functional reads

$$E = \frac{J}{2} \sum_{\langle i,j \rangle} \mathbf{m}_i \cdot \mathbf{m}_j - \frac{D}{2} \sum_{\langle i,j \rangle} \mathbf{d}_{ij} \cdot (\mathbf{m}_i \times \mathbf{m}_j) - K \sum_i (m_i^z)^2 - MB \sum_i m_i^z, \quad (1)$$

where  $\langle i, j \rangle$  denotes the summation over the nearest neighbors,  $\mathbf{m}_i$  is the unit vector in the direction of the magnetic moment on site  $i$ ,  $J$  and  $D$  are the exchange and DMI constants, respectively,  $K$  is the anisotropy constant,  $B$  is the magnetic field, and  $M$  is the magnitude of on-site magnetic moment. Both the anisotropy and external field are perpendicular to the AFM film. The DMI vectors  $\mathbf{d}_{ij}$  point perpendicular to the bond connecting sites  $i$  and  $j$ . Eq. (1) defines a multidimensional energy surface as a function of orientation of magnetic moments, where in a certain parameter range the local minima corresponding to Néel-type skyrmions appear [33].

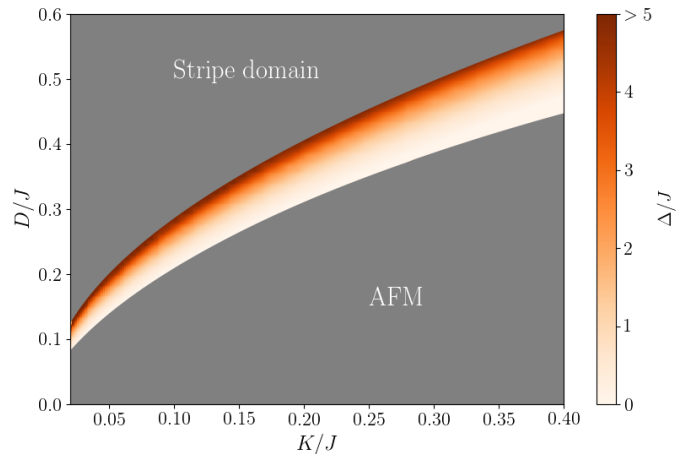


FIG. 1: AFM skyrmion stability diagram at zero temperature. The skyrmion is stable within the colored region, having the tendency towards stripe phase above the upper critical line and towards the uniform AFM (ground) state below the lower critical line. The colors within the AFM skyrmion existence region code the magnitude of the activation energy  $\Delta$  of the skyrmion decay to the uniform AFM state. The activation energy  $\Delta$  characterizes the skyrmion lifetime by means of the Arrhenius law, Eq. (2).

The lifetime of AFM skyrmions,  $\tau(T)$ , is calculated using harmonic transition state theory for magnetic systems [48]. Similar stochastic approaches are employed in various branches of condensed matter physics for the evaluation of decay rate of a metastable state [49, 50]. The theory predicts an Arrhenius expression for the lifetime as a function of temperature  $T$ ,

$$\tau(T) = \frac{1}{\nu(T)} e^{\Delta/k_B T}. \quad (2)$$

Here the activation energy  $\Delta$  is given by the energy difference between the skyrmion-state local minimum and relevant saddle point located on the minimum energy path connecting the skyrmion configuration with the uniform AFM phase. The attempt frequency  $\nu(T)$  is defined by the curvature of the energy surface at the saddle point and at the skyrmion-state minimum. It acquires power-law temperature dependence due to zero-energy modes corresponding to free translational motion of the skyrmion structure [51, 52]. The identification of minimum energy paths and corresponding saddle points on the energy surface, an essential part of the stability analysis within the harmonic transition state theory, is carried out using the geodesic nudged elastic band method [53].

*Stability diagram.* The energy functional of Eq. (1) can be minimized numerically for different initial configurations to establish the existence of local minima. For the AFM model with  $J > 0$  we investigate the stability of an isolated AFM skyrmion in the absence of external field ( $B = 0$ ). The results of this analysis are shown in Fig. 1.

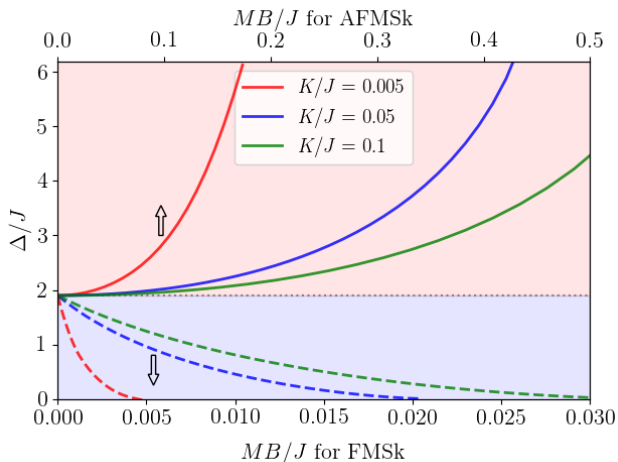


FIG. 2: Activation energy  $\Delta$  as a function of applied magnetic field  $B$  for AFM (solid lines) and FM (dashed lines) skyrmions (Sk) for several values of the anisotropy constant  $K$ . The corresponding dimensionless quantities are  $\Delta/J$  and  $MB/J$ . Note the drastic difference in the magnetic field ranges for the AFMSk and FMSk, respectively. Here  $M$  is the magnetic moment per lattice site. For each value of  $K$ , the DMI constant was chosen so that the activation energies for the skyrmion decay coincide at zero field.

The isolated skyrmion remains metastable in a colored band in the  $D$ - $K$  parameter space. The lower bound of the band corresponds to the vanishing skyrmion size which eventually becomes unstable. When the values of parameters  $K$  and  $D$  approach the upper bound in Fig. 1, the skyrmion expands indefinitely gradually adjusting its shape to the symmetry of the chosen lattice model, that is, developing a square shape. The upper bound indicates a transformation of a square-like skyrmion to a stripe domain, for which it is energetically favorable to increase the length of the domain wall indefinitely. The size of metastable stripe domains diverges and is defined by the system size.

The boundary between the skyrmion phase and the stripe domain phase can be obtained analytically within the micromagnetic continuous model. As described above, when approaching the upper boundary from below the size of the skyrmion increases without limits. For a sufficiently large skyrmion size, its energy coincides with that of a domain wall of length equal to the skyrmion perimeter, for which the analytical results are already established [54]. In zero magnetic field, we estimate

$$D_c(K) = \frac{4}{\pi} \sqrt{\frac{KJ}{2}}, \quad (3)$$

where  $D_c$  gives the critical DMI strength along the upper skyrmion existence bound [cf. Eqs. (14) and (26) in Ref. 54 for the domain wall].

A magnetic field has a nontrivial effect on the AFM

skyrmion stability. Figure 2 shows the barrier for the AFM skyrmion decay as a function of applied field strength. These results are in sharp contrast with the field dependence of the FM skyrmion ( $J < 0$ ), where the barrier quickly decreases with the field [52]. On contrary, for the AFM skyrmion ( $J > 0$ ) the energy barrier is significantly enhanced, but the effect manifests itself at much larger fields.

To gain a further insight into this unusual behavior of AFM skyrmions, it is instructive to estimate the skyrmion radius by minimizing the energy functional in the presence of magnetic field. Such an estimate can be obtained analytically within the micromagnetic continuum model for the Néel vector [55], using a trial skyrmion solution for the azimuthal angle  $\theta(r) = \pi(1 - r/R)$  with  $0 < r < R$ , where the parameter  $R$  is associated with the skyrmion radius [56]. This analysis gives the minimized radius  $R_0 = \pi JD / (JK - M^2 B^2 / 16)$ , thus showing that the AFM skyrmion size increases with the field. It is consistent with the field dependence of the energy barrier observed in the numerical simulations, since larger skyrmions correspond to larger energy barriers, as discussed above. One can arrive at the same conclusion from another perspective. It has been shown in [55] that in the continuous model the energy functional of the AFM skyrmion system at an arbitrary applied field is equivalent to that of the FM counterpart at zero field, where the anisotropy parameter is effectively reduced by  $M^2 B^2 / (16J)$ . Therefore, the enhancement of the energy barrier for the AFM skyrmions in magnetic field can be understood by the renormalization of the anisotropy constant in the FM-skyrmion decay problem. Indeed, the decrease in the energy barrier for the FM skyrmion decay with the anisotropy strength has recently been confirmed in Ref. [57].

We furthermore analyze the distribution of energy barriers  $\Delta$  that have to be overcome for an isolated AFM skyrmion to decay into the uniform AFM state (see Fig. 1). As expected, the barrier height increases monotonically as one moves from the lower stability boundary to the upper one, however the rate of this increase is not constant. In particular, the barrier demonstrates weak dependence on the material parameters in the wide region close to the lower boundary, where the barrier is rather small. The dependences on  $K$  and  $D$  become more pronounced as one approaches the upper stability boundary: the barrier increases rapidly, enhancing the stability of large skyrmions. These results suggest that even at low temperatures sufficiently small skyrmions may be easily destroyed by thermal fluctuations in a large lower portion of the stability diagram, thus significantly reducing the AFM skyrmion stability region at finite temperatures. Given the exponential dependence of the lifetime on energy barrier, it is expected that AFM skyrmions are stable at long time scales in the region close to the upper stability boundary described by Eq. (3). Such AFM

skyrmions may indeed be detected on the experimentally relevant time scales.

*AFM skyrmion lifetime.* Perhaps, the most crucial issue that needs to be addressed for the direct implication of magnetic skyrmions in real devices is its stability with respect to thermal fluctuations [33]. In real systems, the magnetic moments are localized on sites of a discrete lattice and topological arguments are no more straightforwardly applicable. The metastable and ground states of the energy functional are separated by a finite activation energy  $\Delta$ , which in general would also depend on the lattice parameters. The energy surface we study is described by the spin Hamiltonian of Eq. (1) on a square lattice. According to Eq. (2), the temperature dependence of skyrmion lifetime is primarily determined by the activation energy that has to be overcome by a skyrmion to lose its topological charge and decay into the AFM ground state.

Our results for the skyrmion lifetime at finite temperatures are presented in Fig. 3 for a fixed value of the anisotropy parameter  $K = 0.1J$ . As seen from Fig. 3, the lifetime is sufficiently small in the region of small  $D$ . This is in good agreement with the values of the barrier  $\Delta$  at the lower bound of the region in Fig. 1. To the contrary, for larger  $D$  (the upper bound in Fig. 1), the topological charge is hard to lose due to the large skyrmion size, hence the lifetime is maximal. Since the lifetime in Fig. 3 is given in units of intrinsic precession time,  $\tau_0 = M/(\gamma J)$ , it allows us to estimate it for concrete material parameters. By taking parameters, which are similar to those used in [33],  $J = -9.2 \times 10^{-22}$  J,  $D = 5.5 \times 10^{-23}$  J, and  $K = 4.6 \times 10^{-24}$  J, one deduces that AFM skyrmions may be stable on the timescales of seconds at temperatures 25 – 30 K (or milliseconds for temperatures in the range of 50 – 65 K), and therefore can in principle be detected with SP-STM technique.

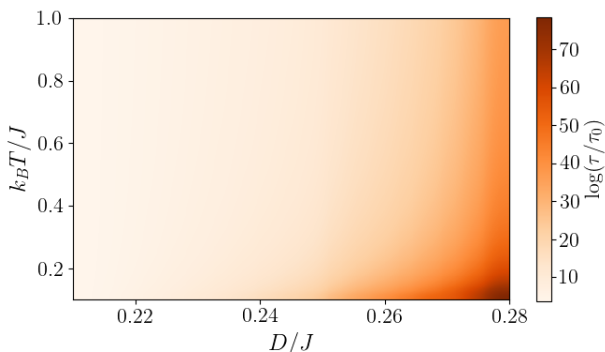


FIG. 3: Lifetime of AFM skyrmion as a function of DMI strength  $D$  and temperature  $T$  at a fixed anisotropy strength  $K/J=0.1$ . The characteristic time scale  $\tau_0$  is given by  $\tau_0 = M/(\gamma J)$ , where  $\gamma$  is the gyromagnetic ratio.

*Conclusions.* We have explored the stability and lifetimes of AFM skyrmions at finite temperatures within

harmonic transition state theory formalism. The non-uniform distribution of energy barriers for the skyrmion decay has been shown to lead to a significant reduction of the AFM skyrmion stability region at finite temperatures. The results of the lifetime analysis reveal that at finite magnetic fields one can find a critical temperature below which AFM skyrmion becomes more stable than its FM counterpart. Surprisingly, in sharp contrast to FM skyrmions, which rapidly become unstable with increasing magnetic field, its AFM counterparts demonstrate higher stability in finite magnetic fields. These fields may be large for usual AFMs (corresponding to roughly 50 – 100 Tesla), however the critical fields above which the AFM skyrmion becomes more stable may be rather easily achieved in the AFMs with weak AFM exchange. Furthermore, we have calculated the AFM skyrmion lifetimes to be in the range of milliseconds for reasonable temperature range (50 – 65 K), thus demonstrating that AFM skyrmions can be experimentally observed and employed in spintronic applications. This temperature range for AFM skyrmions can be increased by increasing further the magnetic field.

*Acknowledgements.* The authors thank V. M. Uzdin and H. Jónsson for helpful discussions. P. F. B. acknowledges support from the Icelandic Research Fund (Grant No. 163048-052). P. B., D. Y., D. R. G., and M. T. acknowledge support from the Russian Science Foundation under the Project 17-12-01359. The work of M. T. was partially supported by ICC-IMR, Tohoku University. O. A. T. acknowledges support by the Grants-in-Aid for Scientific Research (Grants No. 25247056, No. 17K05511, and No. 17H05173) from the Ministry of Education, Culture, Sports, Science and Technology (MEXT) of Japan and by JSPS and RFBR under the Japan-Russia Research Cooperative Program.

\* Electronic address: olegt@imr.tohoku.ac.jp

- [1] V. G. Makhankov, Y. P. Rybakov, and V. I. Sanyuk, in *The Skyrme Model. Springer Series in Nuclear and Particle Physics.* (Springer, Berlin, Heidelberg, 1993).
- [2] T. H. R. Skyrme, Nucl. Phys. **31**, 556 (1962).
- [3] A. N. Bogdanov and D. A. Yablonskii, Sov. Phys. JETP **68**, 101 (1989).
- [4] X. Z. Yu, Y. Onose, N. Kanazawa, J. H. Park, J. H. Han, Y. Matsui, N. Nagaosa, and Y. Tokura, Nature **465**, 901 (2010).
- [5] S. Heinze, K. von Bergmann, M. Menzel, J. Brede, A. Kubetzka, R. Wiesendanger, G. Bihlmayer, and S. Blugel, Nat Phys **7**, 713 (2011).
- [6] N. Romming, C. Hanneken, M. Menzel, J. E. Bickel, B. Wolter, K. von Bergmann, A. Kubetzka, and R. Wiesendanger, Science **341**, 636 (2013).
- [7] N. Nagaosa and Y. Tokura, Nature Nanotech. **8**, 899 (2013).
- [8] M. Mochizuki and Y. Watanabe, Appl. Phys. Lett. **107**,

- 082409 (2015).
- [9] J. Müller, A. Rosch, and M. Garst, *New J. Phys.* **18**, 065006 (2016).
- [10] K. Everschor-Sitte, M. Sitte, T. Valet, A. G. Abanov, and J. Sinova, *New Journal of Physics* (2017), URL <http://iopscience.iop.org/10.1088/1367-2630/aa8569>.
- [11] A. De Lucia, K. Litzius, B. Krüger, O. A. Tretiakov, and M. Kläui, *Phys. Rev. B* **96**, 020405 (2017).
- [12] A. Rosch, *Nature Nanotech.* **8**, 160 (2013).
- [13] A. Rosch, *Nature Nanotech.* **12**, 103 (2017).
- [14] X. Z. Yu, N. Kanazawa, Y. Onose, K. Kimoto, W. Z. Zhang, S. Ishiwata, Y. Matsui, and Y. Tokura, *Nature Mater.* **10**, 106 (2011).
- [15] A. O. Leonov, Y. Togawa, T. L. Monchesky, A. N. Bogdanov, J. Kishine, Y. Kousaka, M. Miyagawa, T. Koyama, J. Akimitsu, T. Koyama, et al., *Phys. Rev. Lett.* **117**, 087202 (2016).
- [16] W. Jiang, P. Upadhyaya, W. Zhang, G. Yu, M. B. Jungfleisch, F. Y. Fradin, J. E. Pearson, Y. Tserkovnyak, K. L. Wang, O. Heinonen, et al., *Science* **349**, 283 (2015).
- [17] C. Moreau-Luchaire, C. Moutas, N. Reyren, J. Sampaio, C. A. F. Vaz, N. Van Horne, K. Bouzehouane, K. Garcia, C. Deranlot, P. Warnicke, et al., *Nature Nanotech.* **11**, 444 (2016).
- [18] A. Soumyanarayanan, M. Raju, A. L. Gonzalez Oyarce, A. K. C. Tan, M.-Y. Im, A. P. Petrovic, P. Ho, K. H. Khoo, M. Tran, C. K. Gan, et al., *Nature Mater.* (2017).
- [19] S. Woo, K. Litzius, B. Kruger, M.-Y. Im, L. Caretta, K. Richter, M. Mann, A. Krone, R. M. Reeve, M. Weigand, et al., *Nature Mater.* **15**, 501 (2016).
- [20] B. Dupé, G. Bihlmayer, M. Böttcher, S. Blügel, and S. Heinze, *Nat. Commun.* **7** (2016).
- [21] K. Litzius, I. Lemes, B. Kruger, P. Bassirian, L. Caretta, K. Richter, F. Buttner, K. Sato, O. A. Tretiakov, J. Forster, et al., *Nature Phys.* **13**, 170 (2017).
- [22] W. Jiang, X. Zhang, G. Yu, W. Zhang, X. Wang, M. Benjamin Jungfleisch, J. E. Pearson, X. Cheng, O. Heinonen, K. L. Wang, et al., *Nat. Phys.* **13**, 123 (2017).
- [23] A. Fert, V. Cros, and J. Sampaio, *Nat. Nano.* **8**, 152 (2013).
- [24] R. Tomasello, E. Martinez, R. Zivieri, L. Torres, M. Carpentieri, and G. Finocchio, *Sci. Rep.* **4** (2014).
- [25] W. Koshiybae, Y. Kaneko, J. Iwasaki, M. Kawasaki, Y. Tokura, and N. Nagaosa, *Jpn. J. Appl. Phys.* **54**, 053001 (2015).
- [26] W. Kang, Y. Huang, C. Zheng, W. Lv, N. Lei, Y. Zhang, X. Zhang, Y. Zhou, and W. Zhao, *Sci. Rep.* **6** (2016).
- [27] A. A. Thiele, *Phys. Rev. Lett.* **30**, 230 (1973).
- [28] O. A. Tretiakov, D. Clarke, G.-W. Chern, Y. B. Bazaliy, and O. Tchernyshyov, *Phys. Rev. Lett.* **100**, 127204 (2008).
- [29] D. J. Clarke, O. A. Tretiakov, G.-W. Chern, Y. B. Bazaliy, and O. Tchernyshyov, *Phys. Rev. B* **78**, 134412 (2008).
- [30] K. Everschor, M. Garst, R. A. Duine, and A. Rosch, *Phys. Rev. B* **84**, 064401 (2011).
- [31] J. Iwasaki, M. Mochizuki, and N. Nagaosa, *Nat Nano* **8**, 742 (2013).
- [32] I. A. Ado, O. A. Tretiakov, and M. Titov, *Phys. Rev. B* **95**, 094401 (2017).
- [33] J. Barker and O. A. Tretiakov, *Phys. Rev. Lett.* **116**, 147203 (2016).
- [34] X. Zhang, Y. Zhou, and M. Ezawa, *Sci. Rep.* **6** (2016).
- [35] X. Zhang, Y. Zhou, and M. Ezawa, *Nat. Commun.* **7** (2016).
- [36] H. Velkov, O. Gomonay, M. Beens, G. Schwiete, A. Brataas, J. Sinova, and R. A. Duine, *New J. Phys.* **18**, 075016 (2016).
- [37] B. Göbel, A. Mook, J. Henk, and I. Mertig, *Phys. Rev. B* **96**, 060406 (2017).
- [38] P. M. Buhl, F. Freimuth, S. Blügel, and Y. Mokrousov, *Phys. Status Solidi Rapid Res. Lett.* **11**, 1700007 (2017).
- [39] C. A. Akosa, O. A. Tretiakov, G. Tatara, and A. Manchon, arXiv:1709.02931 (2017).
- [40] K. M. D. Hals, Y. Tserkovnyak, and A. Brataas, *Phys. Rev. Lett.* **106**, 107206 (2011).
- [41] E. G. Tveten, A. Qaiumzadeh, O. A. Tretiakov, and A. Brataas, *Phys. Rev. Lett.* **110**, 127208 (2013).
- [42] O. Gomonay, T. Jungwirth, and J. Sinova, *Phys. Rev. Lett.* **117**, 017202 (2016).
- [43] D. R. Rodrigues, K. Everschor-Sitte, O. A. Tretiakov, J. Sinova, and A. Abanov, *Phys. Rev. B* **95**, 174408 (2017).
- [44] T. Jungwirth, X. Marti, P. Wadley, and J. Wunderlich, *Nature Nanotech.* **11**, 231 (2016).
- [45] P. Wadley, B. Howells, J. Železný, C. Andrews, V. Hills, R. P. Campion, V. Novák, K. Olejník, F. Maccheronzi, S. S. Dhesi, et al., *Science* **351**, 587 (2016).
- [46] A. H. MacDonald and M. Tsoi, *Philosophical Transactions of the Royal Society of London A: Mathematical, Physical and Engineering Sciences* **369**, 3098 (2011).
- [47] R. Wiesendanger, *Rev. Mod. Phys.* **81**, 1495 (2009).
- [48] P. F. Bessarab, V. M. Uzdin, and H. Jónsson, *Phys. Rev. B* **85**, 184409 (2012).
- [49] O. A. Tretiakov, T. Gramespacher, and K. A. Matveev, *Phys. Rev. B* **67**, 073303 (2003).
- [50] O. A. Tretiakov and K. A. Matveev, *Phys. Rev. B* **71**, 165326 (2005).
- [51] H.-B. Braun, *Phys. Rev. B* **50**, 16501 (1994).
- [52] P. F. Bessarab, G. P. Müller, I. S. Lobanov, F. N. Rybakov, N. S. Kiselev, H. Jónsson, V. M. Uzdin, S. Blügel, L. Bergqvist, and A. Delin, arXiv:1706.07173 (2017).
- [53] P. F. Bessarab, V. M. Uzdin, and H. Jónsson, *Comput. Phys. Commun.* **196**, 335 (2015).
- [54] A. N. Bogdanov, U. K. Röbner, M. Wolf, and K.-H. Müller, *Phys. Rev. B* **66**, 214410 (2002).
- [55] R. Keesman, M. Raaijmakers, A. E. Baerends, G. T. Barkema, and R. A. Duine, *Phys. Rev. B* **94**, 054402 (2016).
- [56] A. Bogdanov and A. Hubert, *J. Magn. Magn. Mater.* **138**, 255 (1994).
- [57] D. Stosic, J. Mulkers, B. Van Waeyenberge, T. B. Luderemir, and M. V. Milošević, *Phys. Rev. B* **95**, 214418 (2017).